AUT Journal of Electrical Engineering
10.22060/EEJ.2025.24519.5721

An Improved P300-based Brain-Computer Interface using Tensor Methods for Patients with Amyotrophic Lateral Sclerosis

Mozhgan Sanjarani [1], Mohammad Pooyan [2,*] , Farzad Fatehi[3]

[1] Faculty of Electrical, Biomedical and Mechatronics Engineering, Qazvin Branch, Islamic Azad University, Qazvin, Iran

[2] Biomedical Engineering Department, Engineering Faculty, Shahed University, Tehran, Iran

[3] Neuromuscular Research Center, Shariati Hospital, Tehran University of Medical Sciences, Tehran, Iran

[*] Corresponding Author, Email: pooyan@shahed.ac.ir

Abstract

Amyotrophic Lateral Sclerosis (ALS) is a progressive neurological disorder with no fully effective treatment currently available. In this study, a novel tensor-based feature reduction method, Higher Order Spectral Regression Discriminant Analysis (HOSRDA), is proposed to enhance Brain-Computer Interface (BCI) performance in individuals with ALS. HOSRDA extends the principles of Spectral Regression Discriminant Analysis (SRDA) to handle multi-dimensional EEG data, effectively addressing the challenges of high-dimensionality and ill-conditioned scatter matrices in the analysis of P300 speller data. This method reduces the dimensionality of EEG signals while preserving class separability, enabling efficient classification using Linear Discriminant Analysis (LDA). Furthermore, HOSRDA leverages a regression framework to address the computationally expensive eigenvalue decomposition of scatter matrices, a challenge faced by traditional methods like HODA, significantly improving computational efficiency. Experiments conducted on EEG data from five ALS patients show that the HOSRDA-LDA model achieves an average character detection accuracy of 84.04%, demonstrating its potential for real-time BCI applications. Compared to traditional methods such as LDA without feature reduction and Support Vector Machine (SVM), HOSRDA outperforms in terms of classification accuracy and computational efficiency, with significantly reduced training times. The HOSRDA method converges in an average of 2.04 seconds over three repetitions, making it highly suitable for online BCI systems. These findings suggest that HOSRDA can improve the accessibility and usability of BCIs for ALS patients, with potential applications extending to broader clinical and real-world settings, without the need for time-consuming training sessions or considering factors like literacy.

Keywords: Brain-computer interface, P300 speller , Higher Order Spectral Regression Discriminant Analysis (HOSRDA), Amyotrophic Lateral Sclerosis (ALS), signal processing

1.Introduction

10.22060/EEJ.2025.24519.5721

The ability to communicate with the surrounding environment, both verbally and behaviorally, is largely dependent on muscle control[1]. In a considerable number of disorders, including motor neuron diseases (MNDs), this control is weakened or lost. MNDs are a group of progressive neurological disorders that destroy motor neurons, which control the activity of skeletal muscles such as walking, breathing, speaking, and swallowing. This group includes some disorders such as amyotrophic lateral sclerosis (ALS), progressive bulbar palsy (PBP), primary lateral sclerosis (PLS), progressive muscular atrophy(PMA), spinal muscular atrophy(SMA), polio and post-polio syndrome (PPS), and infantile paralysis[2]. ALS is a progressive neurological disorder that causes muscle weakness and deterioration. This disorderprogresses gradually and ultimately leads to the patient's death. The exact cause of this disorderis still unknown, but some studies have shown that genetic, environmental, and immune factors may play a role in its development[2]. In some cases, ALS symptoms begin with weakness in specific parts of the body, such as hands or feet[3].Recent studies indicate that approximately 3 to 8 individuals per 100,000 people worldwide are diagnosed with ALS each year[4].

Brain-computer interface (BCI) systems use neurophysiological signals as input commands to control external devices, disregarding motor output and directly transmitting messages from the brain to the computer. Despite the advantages that BCI systems provide, they have shown limitations that include technical and psychological problems, which hinder obtaining optimal performance with each individual[5](Figure 1).

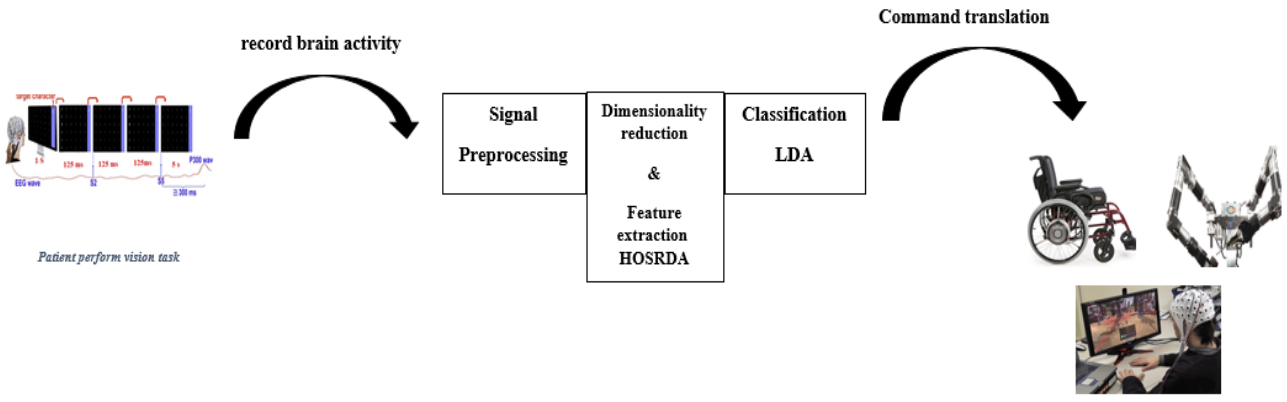

Figure 1. The process that occurs when using a brain-computer interface (BCI)

Unfortunately, communication is just one of the problems in patients withALS. In fact, a wide range of cognitive impairments in the intermediate to severe stages of the disorder has been reported in these patients. The problem arises from the difficulty in performing a standard cognitive battery, which is usually done through tests and self-reports. Clinical evidence shows that sometimes it is almost impossible to accurately assess patients with these tools[6]. The goal of many studies is to provide communication tools that can improve the quality of life of these individuals. BCI systems are a technology that can analyze brain signals for communication with the external environment. For example, controlling a typing robot, controlling a wheelchair to navigate to a desired location, designing care and rehabilitation, and treatment are some examples that this technology can manage[7].

Despite the various methods available for measuring brain activity, almost 80% of used BCI systems are based on electroencephalography (EEG). Specifically, cognitive processes are measured using the average activity of dendritic currents over time using electrodes placed on the scalp with standard settings. In other words, by using single-task experiment settings, specific patterns of individual brain activity can be extracted using EEG analysis by BCI systems[8]. Invasive BCIs use the amplification of one or more neurons and local field potentials, which is usually used for severe or unresponsive disorders due to associated risks. EEG monitoring is one of the most popular measurement tools in BCI applications due to its non-invasiveness, portability, and relatively low cost [9-11].

Event-related potentials (ERP)-based visual BCI is one of the popular BCIs and has received attention[12]. Non-invasive BCIs focus on various parameters of EEG such as frequency oscillation components or brain evoked potentials such as P300, or steady state visual evoked potential (SSVEP)[9]. P300 is a positive deviation that reflects brain activity and provides the extracted pattern in the brain[13]. One of the most famous ERP-based visual BCIs is an oddball pattern speller, which was first introduced by Farwell and Donchin in 1988. In this method, the user focuses on target stimuli that are randomly presented with a sequence of non-target stimuli, and the brain response, P300 event-related potential, is recognized[12]. P300 is a positive deviation that occurs about 250 to 500 milliseconds after an unusual event. However, the time of this response varies depending on factors such as age, task design, and neurological condition. Factors that affect this delay can also reduce BCI performance and make these systems

ineffective or impractical for end-users[13]. However, dissatisfaction among participants has increased because patients have to spend more time and tolerate multiple repetitions to increase system efficiency. To overcome these challenges, researchers need to strike a reasonable balance between time, cost, accuracy, and complexity in designing P300 detection methods[14, 15]. In addition, recent observations show that P300 responses directly affect tissue learning and updating processes as well as memory work processes, classification certainty, and conscious processing[16-22].

Tensor decomposition, as a data analysis method, is much more flexible than matrix-based approaches and is very useful for designing BCIs. Therefore, this study assessed tensor-based methods and the accuracy and speed of classification in these methods to reduce analysis time for ALS patients to use BCIs in the real world without the need for time-consuming training sessions for users and the ability for all users to use them regardless of language and literacy level.

What We Will Present

In our proposed approach, dimensionality reduction and feature extraction will be carried out using tensor-based methods to reduce computational complexity, ensuring high classification accuracy and computational efficiency. The goal is to eliminate training sessions while maintaining high classification accuracy and utilizing Brain-Computer Interfaces (BCI) for the general public, regardless of age, gender, literacy level, or disease progression. This gap is what we aim to address with our approach. An LDA (Linear Discriminant Analysis) classifier is employed to reduce computational complexity.

In the second section, previous research in this field will be discussed. The third section will examine the challenges and limitations ahead. The fourth section will cover data recording methods, the participants involved in the study, and the proposed methods. Section five will present the results along with an analysis. The findings will be discussed and compared with previous works in section six, and finally, section seven will provide the conclusion.

2.Related Work

In many studies, efforts have been made to use tensor-based methods for dimensionality reduction and feature extraction, yielding significant results. Brain-Computer Interfaces (BCIs) based on the P300 component rely on the detection of event-related potentials (ERPs) in electroencephalographic (EEG) signals. has been extensively used for various applications,

including communication, control, and rehabilitation. Feature extraction is a critical step in the design of efficient BCIs, as it determines the quality of the data fed into classification algorithms. Traditional feature extraction methods often flatten EEG data, potentially losing spatial, temporal, and inter-trial relationships. Tensor-based feature extraction methods preserve these multi-dimensional structures, offering a powerful alternative for processing P300 data[23-26].

EEG signals are naturally multi-dimensional, encompassing spatial (electrodes), temporal (time points), and experimental (trials or conditions) domains. Traditional feature extraction methods often involve concatenating these dimensions into a single vector, potentially discarding interrelationships. Recent research advocates for tensor representations to address this limitation. For instance, Cong et al. (2015) emphasized the utility of tensor decomposition in preserving the spatial and temporal dependencies inherent in EEG signals. They demonstrated that tensor representations could improve the accuracy of feature extraction and classification in ERPs[27-29].

Several tensor decomposition methods have been explored in P300 BCIs:

CANDECOMP/PARAFAC (CP) Decomposition: CP decomposition represents a tensor as a sum of rank-one components, enabling the isolation of key spatiotemporal features. Lotte et al. (2018) applied CP decomposition to extract discriminative features from P300 signals, reporting significant improvements in classification accuracy[30].

Tucker Decomposition: This method generalizes principal component analysis (PCA) to tensors, capturing core spatiotemporal patterns while reducing dimensionality. Zubair et al. (2016) implemented Tucker decomposition for EEG tensors, observing enhanced performance in distinguishing target and non-target stimuli[31].

Higher-Order Singular Value Decomposition (HOSVD): HOSVD has been employed for dimensionality reduction in tensor-based EEG analysis. Lu et al. (2020) used HOSVD to extract robust features for P300 classification, achieving notable improvements in computational efficiency[32].

Spatial filtering techniques like Common Spatial Patterns (CSP) are widely used in BCI applications but are typically applied to flattened EEG data. Researchers have extended CSP to tensor frameworks, allowing for the simultaneous optimization of spatial and temporal patterns.

Zhang et al. (2019) proposed tensor CSP methods that leveraged the multi-dimensional structure of EEG data, resulting in improved robustness to noise and artifacts[33].

Wavelet transforms have been integrated with tensor representations to analyze frequency-specific features of P300 responses. Li et al. (2021) employed wavelet tensor analysis to capture the time-frequency characteristics of EEG signals, demonstrating superior classification performance compared to traditional wavelet-based methods[34].

Directly leveraging tensor structures in classification algorithms has shown promise. Tensor-Train Support Vector Machines (TT-SVM) and tensor regression models have been explored for their ability to handle high-dimensional tensor features efficiently. Sun et al. (2022) highlighted the advantages of TT-SVM in reducing the computational complexity of BCI systems without sacrificing accuracy[35].

Comparative studies between tensor-based and traditional feature extraction methods consistently underscore the advantages of tensors in P300 BCIs. For instance, He et al. (2020) compared tensor decomposition methods with PCA and CSP, finding that tensor approaches yielded higher classification accuracy and better generalization across subjects[36].

EEG data naturally contains information on various test conditions, times, frequencies, channels, and more. As a result, tensor tools are widely used for EEG applications, including analyzing brain-computer interfaces, epileptic individuals' EEG, and event-related potentials (ERPs). However, working with high-dimensional EEG data in the matrix domain can limit our ability to leverage all the information provided in each condition and may even introduce interference.Tensor decompositions are effective tools for extracting hidden information and relationships within multidimensional tensor data. Higher Order Discriminant Analysis (HODA) is a popular tensor-based method that extends Linear Discriminant Analysis (LDA), while Spatio-Temporal Discriminant Analysis (STDA) is a specific form of HODA used in P300 data analysis[23, 37, 38].

Spectral Regression Discriminant Analysis (SRDA) is a type of LDA that solves the eigenvalue problem using a set of linear equations. HOSRDA, introduced in 2017 by Jamshidiet al., is a tensor-based method that extends SRDA for analyzing ERPs[39]. HOSRDA utilizes a third-order tensor with time, channel, and test dimensions and transforms the eigenvalue problem into a

regression problem[9]. The High-order spectral regression discriminant analysis (HOSRDA)algorithm requires a stopping point to ensure stability and convergence, which is achieved by maximizing the Fisher ratio. The performance of the system is evaluated using a character detection test to determine the number of correctly detected characters from the test set. The formulation of HOSRDA is expressed as follows, as described previously and the extension of the HODA method introduced by Yan et al. in 2005[40]. HOSRDA with tensor feature reduction method is used for ERP detection[39].

Tensor feature extraction has emerged as a powerful approach for processing.

3. Limitations and challenges

BCIs provide patients with the ability to communicate, significantly improving their quality of life[41]. However, current BCIs face many challenges, such as providing accurate biofeedback to the user[42] Delay: If the delay between the action and its feedback is too long, the patient's ability to learn and improve effective BCI control can be significantly affected[43] Low signal-to-noise ratio[44-46].

The main issue in practical applications is reducing training time, making it suitable for the general public, improving classification accuracy, while simultaneously reducing system complexity and improving response time[47].

Despite the advantages of tensor-based methods, several challenges remain in their application to Brain-Computer Interfaces (BCIs):

Computational Complexity: Tensor operations are computationally intensive, which can hinder their real-time application in BCIs.

Robustness to Noise: Although tensors are effective at preserving multi-dimensional relationships, they may still be vulnerable to noise and artifacts present in EEG data, compromising their reliability.

Standardization: A lack of standardized frameworks and benchmarks for evaluating tensor-based methods limits the ability to consistently assess their performance and comparability across different studies.

To overcome these obstacles, future research must focus on optimizing tensor algorithms for real-time processing, integrating advanced noise-reduction techniques, and exploring hybrid approaches that combine tensor methods with deep learning frameworks.

In parallel, there is a significant gap in optimizing BCI systems for patients with Amyotrophic Lateral Sclerosis (ALS), particularly in the disease's advanced stages, where cognitive impairments complicate the use and assessment of these systems. Traditional cognitive tests and self-reports often fail to provide an accurate baseline for these patients, highlighting the urgent need for more flexible and sophisticated communication tools. Moreover, the extensive BCI training sessions required—sometimes lasting several hours—along with the variability among users, adds further complexity to the issue.

The aim of this research is to address these challenges by exploring tensor-based methods to enhance the accuracy and speed of BCI classification, particularly for event-related potential (ERP)-based visual BCIs. The primary objective is to develop efficient, user-friendly BCI systems through tensor decomposition, offering greater flexibility than traditional matrix-based methods. Ultimately, the goal is to create BCIs that can be effectively used by ALS patients in real-world environments, without the need for extensive training or reliance on language or literacy levels.

This study examines the potential of tensor decomposition techniques in BCI systems, emphasizing their ability to generalize classical matrix-based methods. This approach represents a new frontier in BCI design, particularly for ALS patients. The research aims to improve the accuracy and speed of classification in BCI systems, with a focus on ERP-based visual BCIs, ultimately reducing the time required for analysis. This reduction will make BCIs more viable for real-world use by ALS patients, addressing one of the key limitations of current systems, which often require long training sessions.

4.Materials and Methods

This study was conducted using a comprehensive methodology consisting of seven sections including: patient assessment (details of the ALS patients), P300 stimulation (explaining the visual paradigm), EEG recording(recording details from 32 channels), preprocessing(filtering and

artifact removal steps),feature extraction (using HOSRDA for tensor decomposition), classification(applying LDA on extracted features) and evaluation(presenting the classification accuracy results)**.**

4.1.Patient assessment

This study was conducted on five patients with ALS who referred to Shariati Hospital (Tehran, Iran) and in collaboration with the Rare Diseases Foundation of Iran (RADOIR). This study was approved by the Ethics Committee of the Iran University of Medical Sciences. An informed consent was obtained from all patients. The diagnosis of ALS was made based on clinical, laboratory, and genetic findings. The diagnosis was made using the Awaji criteria for diagnosing ALS, and the patients with probable or definite ALS were recruited[48]. In addition, revised amyotrophic lateral sclerosis functional rating scale (ALSFRS-R) was also used in this study. ALSFRS-R is an assessment tool used to measure the severity of ALS. This score includes 42 questions related to muscle movement, breathing, speech, eating, and running abilities. Each question is evaluated on a scale of 0 to 4, and the total score ranges from 0 to 44, with higher scores indicating less severe disorder and lower scores indicating more severe disorder. ALSFRS-R is usually used in each patient visit to assess disease progress and treatment efficacy. In this study, which was conducted at the National Brain Mapping Laboratory (NBML), the goal was to record the P300 signal and perform offline BCI. None of the patients had prior experience with BCI.

4.2.P300 stimulation

ABCI system based on P300 component detection was used in this study. The P300 speller was used to stimulate the visual evoked potential in the brain. The experiment was conducted in a single session on one day. Participants were asked to control a P300 speller with a 6×6 matrix (Figure 2).

10.22060/EEJ.2025.24519.5721

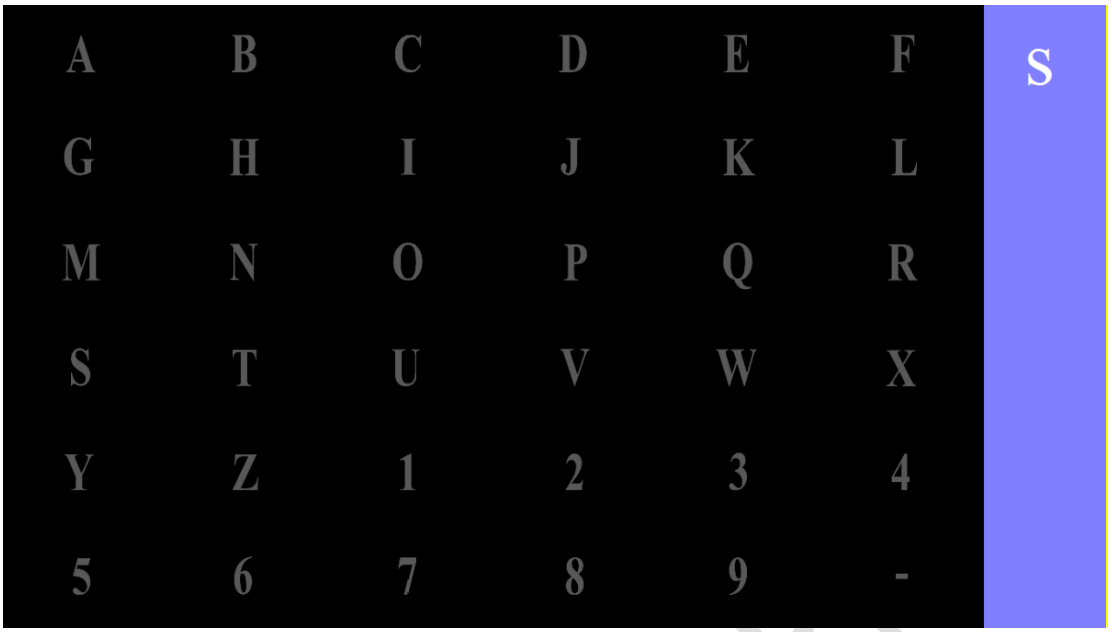

Figure 2. P300 speller used in this study to evaluate patients with amyotrophic lateral sclerosis, displayed on an LCD screen.

EEG recording

The scalp EEG signal was recorded from 32 channels using the international 10-20 system . All electrodes were referenced to the right ear and the left mastoid served as the ground. The sampling rate was 256 Hz(Figure 3).

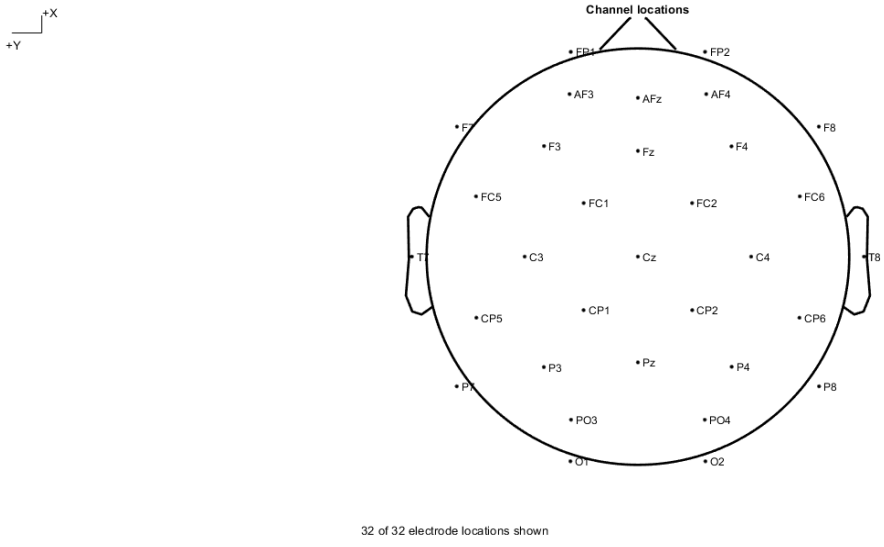

10.22060/EEJ.2025.24519.5721

Figure 3. The electrode placement for recording P300 signals.

The signals and stimuli were prepared and recorded using the BCI2000 framework. Participants were required to spell 7 pre-determined words with 5 characters each in one run using the BCI P300. The characters were displayed in a 6×6 matrix.

The words displayed to patients included Rose, Soup, Mind, Talk, Home, Email, and Sleep. Rows and columns were randomly intensified for 125-msec(using numbers at the beginning of four-letter words). The inter-stimulus interval (ISI) between each intensification was 125-msec, and there was a 250-msecinter-stimulus onset asynchrony (SOA) between each stimulus appearance (Figure 4a).

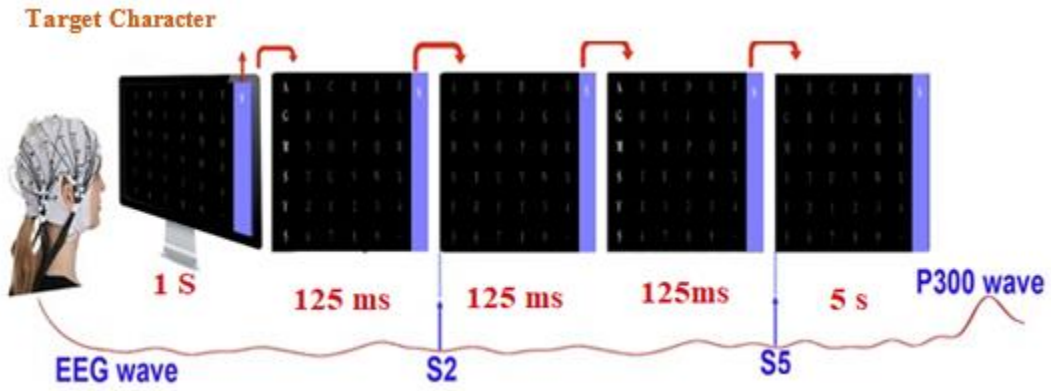

Figure 4a. P300 paradigm stages with their corresponding time intervals.

10.22060/EEJ.2025.24519.5721

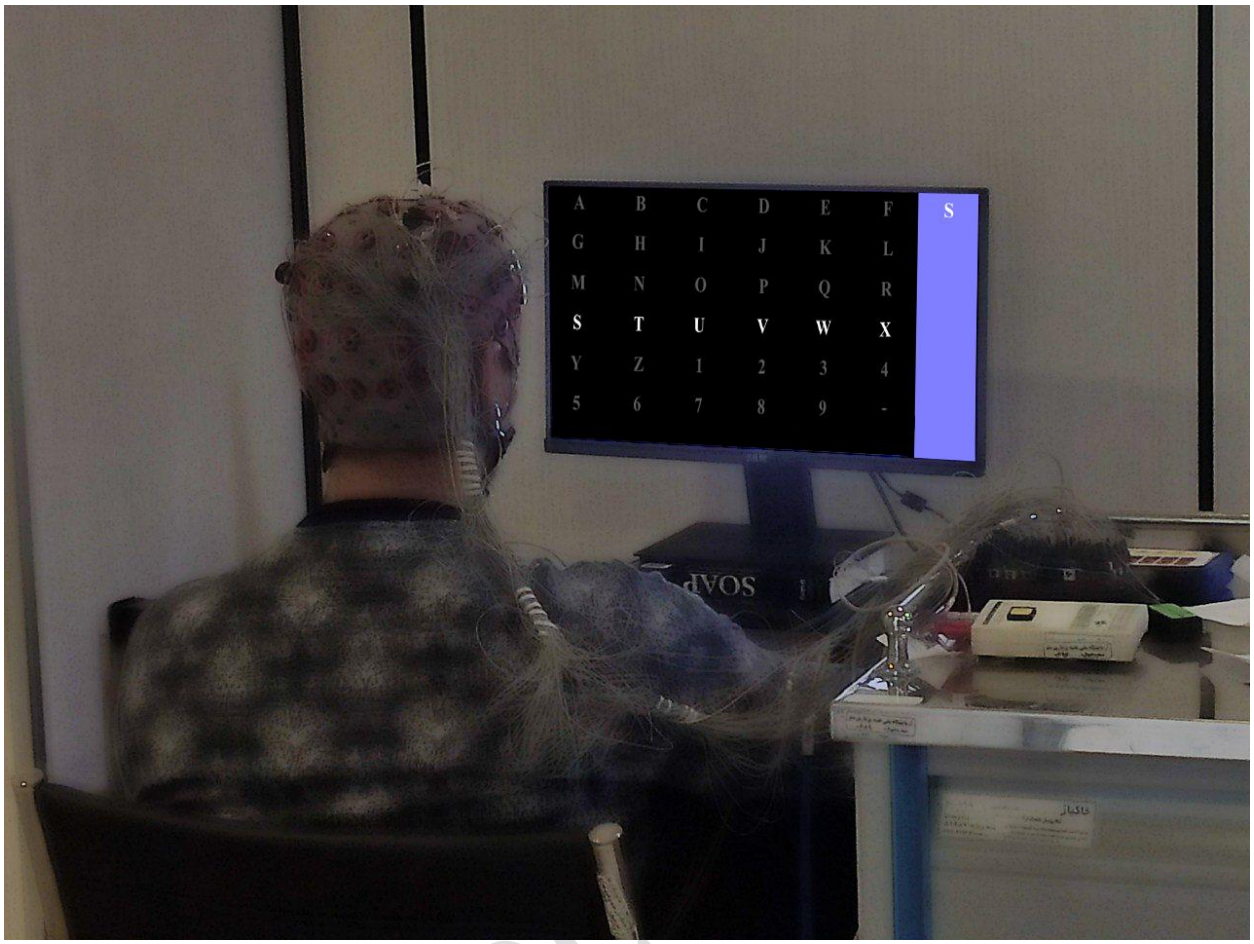

Figure 4b: P300 paradigm with ALS subject

For each trial, rows and columns were intensified 10 times (stimulation repetition). Therefore, each character was intensified 20 times. There was a one-minute break between displaying each word. Participants sat in front of a 15-inch computer screen placed approximately one meter away from them. A single flash was used at the beginning of each trial to aid concentration. The character that the patient was supposed to spell was displayed in the corner of the screen to assist those who were unfamiliar or had limited knowledge of the language.

4.3.Preprocessing

Initially, signal processing was performed using all channels. However, due to minimal differences in results and to reduce processing time, which is crucial for the performance of the brain-computer interface, eight channels were utilized for signal processing. However, due to the minimal

differences in the results and the reduction in processing time, which is crucial for the performance of the brain-computer interface, eight channels (Fz, Cz, Pz, PO3, P3, P4, P7, P8) were used. According to the results of studies [49, 50], these eight channels systematically provide the maximum classifier performance based on various data factors and reference methods. Preprocessing involves three stages: a fourth order low pass Butterworth filter with a cutoff frequency of 10 Hz, a fourth order high pass Butterworth filter with a cutoff frequency of 0.1 Hz and a notch filter at 50 Hz to remove power line noise.

The data is divided into epochs with a length of 1000-msecstarting from each stimulus. Epochs with peak amplitudes higher than 300 microvolts or lower than -300 microvolts are identified as artifacts and removed. Additionally, baseline corrections based on the average EEG activity in the immediate 200 msec after the detection of each epoch are performed. The average waveform shape for target and non-target epochs for each experiment is calculated to obtain the P300 peak amplitude. Specifically, the P300 peak amplitude at Cz is defined as the highest difference between the average waveform shapes of target and non-target epochs in the time interval between 250 to 700 msec .

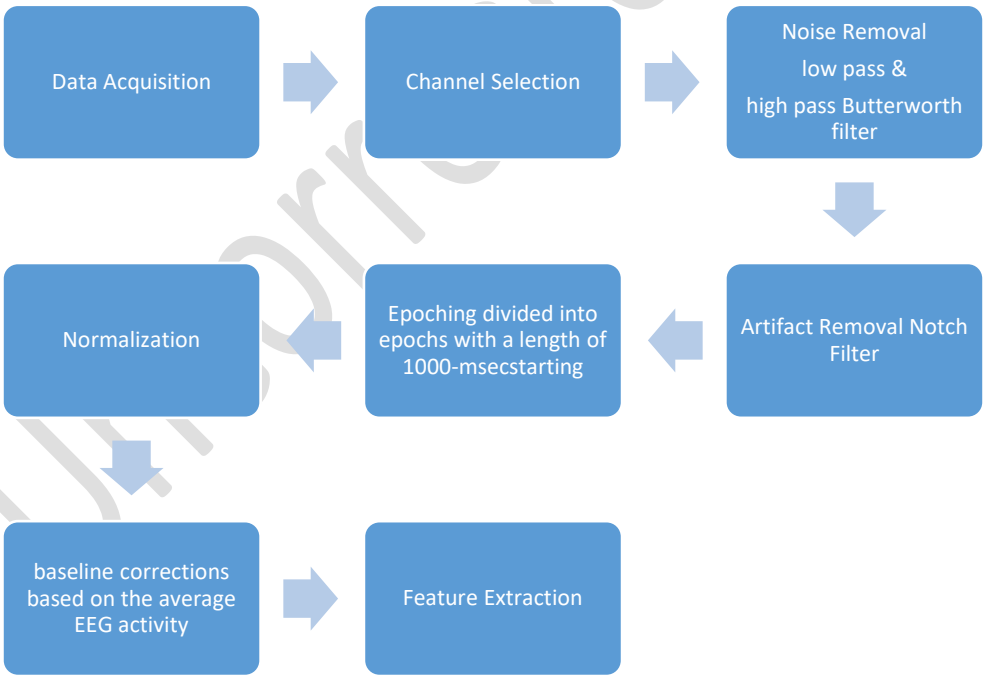

Figure5: Preprocessing Flowchart For EEG Data

4.4.Dimensionality reduction and feature extraction

The method section of the paper uses Higher Order Spectral Regression Discriminant Analysis (HOSRDA), a tensor-based feature reduction technique designed for analyzing Event-Related Potentials (ERP) in EEG data. Here's a summary of the key aspects:

Key Concepts and Components

Tensor Framework:

EEG data, inherently multidimensional, is modeled as tensors to leverage multi-modal information (e.g., channels, time, trials).

Tucker decomposition is used to extract core tensors and factor matrices for dimensionality reduction.

Extension of SRDA:

HOSRDA builds on Spectral Regression Discriminant Analysis (SRDA), converting the eigenvalue problem in Higher Order Discriminant Analysis (HODA) to a regression problem.

This conversion eliminates the need for eigenvalue decomposition, enabling the use of efficient iterative solvers for large datasets.

Mathematical Formulation:

In this paper higher order tensors are shown by calligraphic letters (e.g. $\mathcal{X}$ is a tensor), matrices are denoted by boldface capital letters (e.g. $\boldsymbol{X}$ is a matrix), boldface lower-case letters are used to denote vectors (e.g. $\boldsymbol{x}$ is a vector), and normal letters show scalars (e.g. x or X are scalar).

Ω is the set of all indices of training data samples (e.g. if we have K training data, $\Omega = \{1, \dots, K\}$). The set of indices of data in the c^{th} class with Ω_c and its size by K_c.

$\{x_1, x_2, \dots, x_K\}$ be the set of K data points ($x_i \in \mathbb{R}^m$) from C classes.

Scatter matrices (between-class and within-class) of HODA are redefined in the tensor domain.

The between-class scatter matrix $\boldsymbol{S}_b^{-n}$ is define as follows:

$$\boldsymbol{S}_b^{-n} = \sum_{c=1}^{C} \langle \check{\mathcal{Z}}^{-n(c)}, \check{\mathcal{Z}}^{-n(c)} \rangle_{-n} \qquad (1)$$

Where mode-n product of $\mathcal{Y}$ and $A \in \mathbb{R}^{J_n \times I_n}$ is denoted by $\mathcal{Z}$ and $\mathcal{Y}$ is an N-th order tensors.

10.22060/EEJ.2025.24519.5721

$\mathcal{X}$ is training dataset:

$$\breve{\mathcal{X}}^{(\mathrm{c})} = \sqrt{\mathrm{K_c}\left(\bar{\mathcal{X}}^{\mathrm{c}} - \bar{\bar{\mathcal{X}}}\right)}, \breve{\mathcal{X}} = \mathrm{cat}\left(\mathrm{N}+1, \breve{\mathcal{X}}^{(1)}, \ldots, \breve{\mathcal{X}}^{(\mathrm{C})}\right) \quad (2)$$

U is biasis factors

$\breve{\mathcal{Z}}^{-n(c)} = \breve{\mathcal{X}}^{(c)} \times_{-n} \{U^T\}, \breve{\mathcal{Z}}^{-n} = \breve{\mathcal{X}} \times_{-(n,N+1)} \{U^T\}$ and

$$\bar{\bar{\mathcal{X}}} = \frac{1}{K}\sum_{k=1}^{K} \mathcal{X}^{(k)} \quad (3)$$

$$\bar{\mathcal{X}}^{(c)} = \frac{1}{K_c}\sum_{k\in\Omega_c} \mathcal{X}^{(k)}, c=1,\ldots,C \quad (4)$$

New formulation for between-class scatter matrix of tensor data as follows:

$$\boldsymbol{S}_b^{-n} = \sum_{c=1}^{C} \langle \breve{\mathcal{Z}}^{-n(c)}, \breve{\mathcal{Z}}^{-n(c)} \rangle_{-n} = \sum_{c=1}^{C} \frac{1}{K_c} \langle \sum_{i\in\Omega_c} \mathcal{H}_i^{-n(c)}, \mathcal{H}_i^{-n(c)} \rangle_{-n} \quad (5)$$

Where for $i \in \Omega_c$,$\mathcal{H}_i^{-n(c)} = \left(\mathcal{X}^{(i)} - \bar{\bar{\mathcal{X}}}\right) \times_{-n} \{U^T\}$.Therefore we have:

$$\boldsymbol{S}_b^{-n} = \sum_{c=1}^{C} \frac{1}{K_c} \left(\sum_{i\epsilon\Omega_c} \boldsymbol{H}_{i_{(n)}}^{-n(c)}\right)\left(\sum_{j\epsilon\Omega_c} \boldsymbol{H}_{j_{(n)}}^{-n(c)}\right) = \sum_{c=1}^{C} \boldsymbol{H}_{(n)}^{-n(c)} \boldsymbol{W}^{(c)} \boldsymbol{H}_{(n)}^{-n(c)^T} \quad (6)$$

Where $\mathcal{H}^{-n(c)} = cat\left(N+1, \mathcal{H}_1^{-n(c)}, \ldots, \mathcal{H}_{K_c}^{-n(c)}\right) and\ \boldsymbol{W}^{(c)}$ is a $KP_n \times KP_n$ block matrix whose all blocks are $P_n \times P_n$ identity matrices with $P_n = \prod_{\substack{m=1 \\ m\neq n}}^{N} J_m$ as follows:

$$\boldsymbol{W}^{(c)} = \frac{1}{K_c}\begin{bmatrix} \boldsymbol{I}_{\boldsymbol{p_n}} & \cdots & \boldsymbol{I}_{\boldsymbol{p_n}} \\ \vdots & \ddots & \vdots \\ \boldsymbol{I}_{\boldsymbol{p_n}} & \cdots & \boldsymbol{I}_{\boldsymbol{p_n}} \end{bmatrix} \quad (7)$$

Now if we define $\mathcal{H}^{-n} = cat\left(N+1, \mathcal{H}^{-n(1)}, \ldots, \mathcal{H}^{-n(c)}\right)$ and $\boldsymbol{W} = blockdiag(\boldsymbol{W}^{(1)}, \ldots, \boldsymbol{W}^{(C)})$, the between-class Scatter matrix can be formulated as:

$$\boldsymbol{S}_b^{-n} = \boldsymbol{H}_{(n)}^{-n} \boldsymbol{W} \boldsymbol{H}_{(n)}^{-n^T} \quad (8)$$

In the same way, it can be shown that the within-class scatter matrix can be written as:

$$\boldsymbol{S}_w^{-n} = \boldsymbol{H}_{(n)}^{-n} \boldsymbol{L} \boldsymbol{H}_{(n)}^{-n^T} \quad (9)$$

10.22060/EEJ.2025.24519.5721

Where $\boldsymbol{L} = \boldsymbol{I}_{KP_n} - \boldsymbol{W}\left(\boldsymbol{I}_{KP_n}\ is\ a\ KP_n \times KP_n identity\ matrix\right)$. Thus we can define

$$\boldsymbol{S}_t^{-n} = \boldsymbol{H}_{(n)}^{-n}\boldsymbol{H}_{(n)}^{-n^T} = \boldsymbol{S}_w^{-n} + \boldsymbol{S}_b^{-n} \tag{10}$$

Now instead of solving the optimization problem of HODA:

$$\boldsymbol{U}^{(n)} = argmax \frac{tr\left[\boldsymbol{U}^{(n)^T}\boldsymbol{S}_b^{-n}\boldsymbol{U}^{(n)}\right]}{tr\left[\boldsymbol{U}^{(n)^T}\boldsymbol{S}_w^{-n}\boldsymbol{U}^{(n)}\right]},\ \text{s.t. } \boldsymbol{U}^{(n)^T}\boldsymbol{U}^{(n)} = \boldsymbol{I} \tag{11}$$

We can solve the problem below:

$$\boldsymbol{U}^{(n)} = argmax_{U^{(n)}} \frac{tr\left[\boldsymbol{U}^{(n)^T}\boldsymbol{S}_b^{-n}\boldsymbol{U}^{(n)}\right]}{tr\left[\boldsymbol{U}^{(n)^T}\boldsymbol{S}_t^{-n}\boldsymbol{U}^{(n)}\right]},\ \text{s.t. } \boldsymbol{U}^{(n)^T}\boldsymbol{U}^{(n)} = \boldsymbol{I} \tag{12}$$

A generalized eigenvalue decomposition (GEVD) problem is reformulated into a regression framework:

Instead of solving for eigenvectors, HOSRDA identifies subspace basis factors by solving linear equations iteratively.

$$\boldsymbol{S}_b^{-n}\boldsymbol{u}^{(n)} = \mu\boldsymbol{S}_t^{-n}\boldsymbol{u}^{(n)} \tag{13}$$

If $\boldsymbol{y}$ is eigenvector of $\boldsymbol{W}$ with eigenvalue λ and also we have $\boldsymbol{H}_{(n)}^{-n^T}\boldsymbol{u}^{(n)} = \boldsymbol{y}$, then $\boldsymbol{u}^{(n)}$ is a solution of the GEVD problem (13) with μ=λ. Thus to find the columns of factor matrix $\boldsymbol{U}^{(n)}$, rather than solving a GEVD problem, we can find the J_n leading eigenvectors of $\boldsymbol{W}$ and put them in the columns of matrix $\boldsymbol{Y}$ and then solve the linear system of equations $\boldsymbol{H}_{(n)}^{-n^T}\boldsymbol{U}^{(n)} = \mathbf{Y}$ for $\boldsymbol{U}^{(n)}$.

The eigenvectors of $\boldsymbol{W}$ can be obtained analytically without engendecomposition. Since $\boldsymbol{W}$ is a block-diagonal matrix, its eigenvalues and eigenvectors can be obtained from the eigenvectors and eigenvalues its blocks.

Therefore, we first seek for the eigenvectors/eigenvalues of $\boldsymbol{W}^{(c)}$ for an arbitrary.

Suppose that $\boldsymbol{y}^{(c)}$ is an eigenvectors of $\boldsymbol{W}^{(c)}$ corresponding to eigenvalue λ (i.e. $\boldsymbol{W}^{(c)}\boldsymbol{y}^{(c)} = \lambda\boldsymbol{y}^{(c)}$).

If break $\boldsymbol{y}^{(c)}$ to blocks of vectors of length P_n as $\boldsymbol{y}^{(c)} = \left[\boldsymbol{y}_1^{(c)^T}, \dots, \boldsymbol{y}_{K_c}^{(c)^T}\right]^T$,then we have:

10.22060/EEJ.2025.24519.5721

$$\boldsymbol{W}^{(c)}\boldsymbol{y}^{(c)} = \frac{1}{K_c}\begin{bmatrix} \boldsymbol{I}_{\boldsymbol{p_n}} & \cdots & \boldsymbol{I}_{\boldsymbol{p_n}} \\ \vdots & \ddots & \vdots \\ \boldsymbol{I}_{\boldsymbol{p_n}} & \cdots & \boldsymbol{I}_{\boldsymbol{p_n}} \end{bmatrix}\begin{bmatrix} \boldsymbol{y}_1^{(c)} \\ \dots \\ \boldsymbol{y}_{K_c}^{(c)} \end{bmatrix} \tag{14}$$

$$= \frac{1}{K_c}\begin{bmatrix} \sum_{k=1}^{K_c} \boldsymbol{y}_k^{(c)} \\ \dots \\ \sum_{k=1}^{K_c} \boldsymbol{y}_k^{(c)} \end{bmatrix} = \lambda \begin{bmatrix} \boldsymbol{y}_1^{(c)} \\ \dots \\ \boldsymbol{y}_{K_c}^{(c)} \end{bmatrix} \tag{15}$$

Thus, for each $p = 1, \dots, K_c$ we have $\boldsymbol{y}_p^{(c)} = \frac{1}{\lambda K_c}\sum_{k=1}^{K_c} \boldsymbol{y}_k^{(c)}$. If we define $\boldsymbol{a} \triangleq \boldsymbol{y}_p^{(c)}, \forall p$,it can be easily concluded that $\boldsymbol{a} \triangleq \boldsymbol{y}_p^{(c)} = \frac{1}{\lambda K_c}\boldsymbol{a} = \frac{a}{\lambda}$ and therefore $\lambda = 1$.

For an arbitrary c, it is clear that the rank of $\boldsymbol{W}^{(c)}$ is P_n. Thus, $\boldsymbol{W}^{(c)}$ has P_n eigenvalues of value one with eigenvectors having the form of $\boldsymbol{y}^{(c)} = \left[\boldsymbol{a}_{P_n}^T, \dots, \boldsymbol{a}_{P_n}^T\right]^T$, where $\boldsymbol{a}_{P_n}$ is an arbitrary vector of length P_n.

To find the eigenvectors of $\boldsymbol{W}$, it should be noted that the eigenvalues of a block-diagonal matrix is the union of eigenvalues of its blocks and the eigenvectors of the blocks. Since one is the eigenvalue of all the blocks of $\boldsymbol{W}$, for any set $\{\boldsymbol{y}^{(1)}, \dots, \boldsymbol{y}^{(C)}\}$ of eigenvectors of blocks of $\boldsymbol{W}$, an eigenvectors of $\boldsymbol{W}$ can be defined with the form $\boldsymbol{y} \triangleq \left[\boldsymbol{y}^{(1)^T}, \dots, \boldsymbol{y}^{(c)^T}\right]^T$, corresponding to eigenvalue one. Consequently,we have:

$$\boldsymbol{w}_{\boldsymbol{y}} = \begin{bmatrix} \boldsymbol{W}^{(1)} & 0 & \cdots & 0 \\ 0 & \boldsymbol{W}^{(2)} & \ddots & \vdots \\ \dots & \dots & \cdots & 0 \\ 0 & 0 & 0 & \boldsymbol{W}^{(C)} \end{bmatrix}\begin{bmatrix} \boldsymbol{y}^{(1)} \\ \boldsymbol{y}^{(2)} \\ \dots \\ \boldsymbol{y}^{(C)} \end{bmatrix} \tag{16}$$

$$= \begin{bmatrix} \boldsymbol{W}^{(1)}\boldsymbol{y}^{(1)} \\ \boldsymbol{W}^{(2)}\boldsymbol{y}^{(2)} \\ \dots \\ \boldsymbol{W}^{(C)}\boldsymbol{y}^{(C)} \end{bmatrix} = \begin{bmatrix} \boldsymbol{y}^{(1)} \\ \boldsymbol{y}^{(2)} \\ \dots. \\ \boldsymbol{y}^{(C)} \end{bmatrix} = \boldsymbol{y} \tag{17}$$

Now that we have shown $\boldsymbol{W}$ has CP_n eigenvectors (corresponding to eigenvalue one), which can be constructed using random vectors, the factor matrices of Tucker decomposition can be obtained through solvin a linear system of equations (i.e.$\boldsymbol{H}_{(n)}^{-n^T}\boldsymbol{U}^{(n)} = \boldsymbol{Y}\ for\ \boldsymbol{U}^{(n)}$).

Algorithm Workflow:

10.22060/EEJ.2025.24519.5721

Initialize factor matrices for the tensor decomposition.

Compute the scatter matrices and solve the GEVD problem iteratively using regression.

Perform Gram-Schmidt orthogonalization to ensure orthonormality of the factor matrices.

Stop the iterations when the Fisher ratio (class separability) converges.

Optimization:

Regularization is introduced to handle ill-conditioned scatter matrices and improve stability.

Iterative solvers like LSQR are recommended to reduce computational cost, especially in high-dimensional or small-sample-size (SSS) scenarios.

HOSRDA is a tensor-based feature reduction technique designed to handle multidimensional data (like EEG) by extending the principles of Spectral Regression Discriminant Analysis (SRDA) to tensors. The method aims to efficiently identify low-dimensional subspaces where class separability is maximized.

To use the Standard Linear Discriminant Analysis (LDA) classifier, we face two main challenges: the computational cost of eigenvalue decomposition and conditioned scatter matrices. These challenges need to be addressed in order to solve the issues SRDA reformulates the eigenvalue decomposition in LDA as a regression problem, avoiding computational challenges. HOSRDA extends this idea to tensors for higher-order data.

Tensors are multi-dimensional arrays that naturally represent data with multiple modes (e.g., time, frequency, trials, channels in EEG data).

A tensor $\boldsymbol{Y} \in \mathbb{R}^{I_1 \times \ldots \times I_N}$ represents multi-dimensional data.

Mode-n Matricization: The tensor $\boldsymbol{Y}$ is unfolded into a matrix $Y^{(n)}$ by rearranging its entries along mode n.

Mode-n Product:

$$\boldsymbol{Z} = \boldsymbol{Y} \times_{\boldsymbol{n}} \boldsymbol{A} \qquad (18)$$

Here, $\boldsymbol{Z}$ result from multiplying $\boldsymbol{Y}$ along its $\boldsymbol{n-th}$ mode by a matrix $\boldsymbol{A}$.

10.22060/EEJ.2025.24519.5721

Tucker decomposition is used to reduce tensor dimensionality . Tucker decomposition breaks a tensor Y into a smaller core tensor G and a set of factor matrices$\{U^{(n)}\}$:

$$\boldsymbol{Y \approx G \times_1 U^{(1)} \times_2 \ldots \times_N U^{(N)}} \quad (19)$$

$U^{(n)}$ are orthogonal matrices representing the subspace basis along mode n.

The method defines class scatter matrices in tensor form:

The **between-class scatter matrix**:

$$S_{\mathrm{b}}^{-\mathrm{n}} = H_{(n)}^{-n} W H_{(n)}^{-n^T} \quad (20)$$

Where:

$H_{(n)}^{-n}$: The mode-n unfolded tensor of class means projected onto the subspace.

W: A block-diagonal weight matrix based on class sizes.

The **within-class scatter matrix**:

$$S_w^{-n} = H_{(n)}^{-n} L H_{(n)}^{-n^T} \quad (21)$$

$L = I - W$: *A* complement of the weight matrix W.

Therefore, we have total scatter matrix:

$$S_t^{-\mathrm{n}} = H_{(n)}^{-n} L H_{(n)}^{-n^T} = S_w^{-n} + S_b^{-n} \quad (22)$$

Generalized Eigenvalue Problem (GEVP):

The optimization objective of HODA is maximizing class separability:

$$U^{(\mathrm{n})} = \mathrm{argmax}_{\mathrm{U}^{(\mathrm{n})}} \frac{\mathrm{tr}\left[\mathrm{U}^{(\mathrm{n})^{\mathrm{T}}} \mathrm{S}_{\mathrm{b}}^{-\mathrm{n}} \mathrm{U}^{(\mathrm{n})}\right]}{\mathrm{tr}\left[\mathrm{U}^{(\mathrm{n})^{\mathrm{T}}} \mathrm{S}_{\mathrm{t}}^{-\mathrm{n}} \mathrm{U}^{(\mathrm{n})}\right]} \quad (23)$$

This reduces to solving:

$$\boldsymbol{S_b^{-n} u = \lambda S_t^{-n} u}$$

Reformulation via regression:

10.22060/EEJ.2025.24519.5721

HOSRDA avoids direct eigenvalue decomposition by reformulating the problem:

Given $H_{(n)}^{-n}$ solve:

$$H_{(n)}^{-n^T} U^{(n)} = Y \qquad (24)$$

Here, Y contains eigenvectors of W.

This is a linear regression problem, solved iteratively, avoiding the computational cost and instability of eigenvalue decomposition.

Stopping Criterion

To ensure convergence, the algorithm stops when the Fisher ratio stabilizes:

$$Error = |Fisher\ Ratio(iteration\ i) - Fisher\ Ratio(iterationi - 1)| < \varepsilon \qquad (25)$$

Summary of Formula Roles

- **Scatter matrices** quantify data spread between and within classes.
- **GEVP** defines the optimal subspace for maximizing class separability.
- **Regression reformulation** solves the problem efficiently without eigenvalue decomposition.
- **Stopping criterion** ensures stability and convergence of the algorithm.

Each formula is tailored to balance computational efficiency with accurate feature reduction, especially in tensorial data.

Formula Context

To aid in understanding the mathematical formulations presented, this section briefly explains the context and meaning of the key equations:

the Dimensionality Reduction and Feature Extraction section describe the process of extending Linear Discriminant Analysis (LDA) to handle tensor data through Higher Order Spectral Regression Discriminant Analysis (HOSRDA). These depict extracting the between-class and within-class scatter matrices from the multilayered tensor input data.

10.22060/EEJ.2025.24519.5721

the optimization problem to determine the projection matrices that maximize class separation.

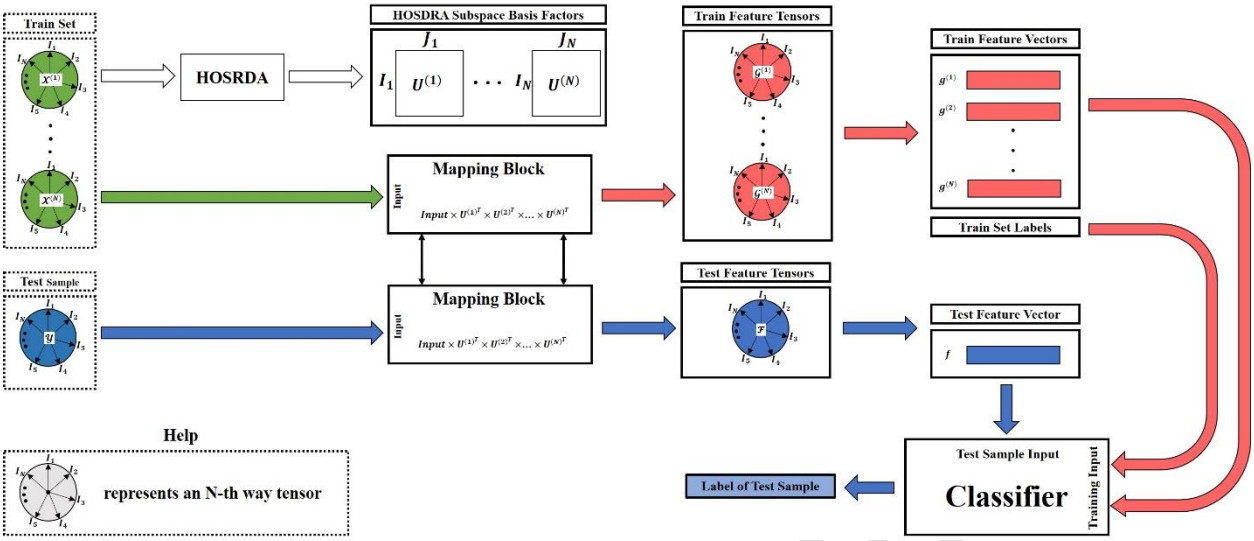

Figure 6: Block diagram of feature reduction classification with higher order spectral regression discriminant analysis (HOSRDA)

As depicted in the block diagram, the training data is first mapped into HOSRDA subspaces using bias factor matrices. From there, the data is transformed into feature vectors using either kernel tensors or feature tensors. These vectors are then simultaneously fed into the classifier block. The same process is used for the test data, which is also mapped and transformed into feature vectors before being inputted into the classifier block. The test data is eventually labeled to complete the process.

Summary of Application

HOSRDA is applied to EEG data from a P300 speller:

- Data is tensorized (channels × time samples × trials).
- HOSRDA reduces the tensor to a lower-dimensional representation while preserving class separability.
- An LDA classifier is applied to the reduced features for classification.

4.5.Classification

Linear Discriminant Analysis (LDA)

10.22060/EEJ.2025.24519.5721

LDA is used for the classification. For this purpose, a linear combination W of features X provides a decision boundary in the form of $W^TX+C=0$ for threshold C. The weights W are found by considering the two multivariate normal distributions of classes with means μ1 and μ2 and covariance's C1 and C2, which maximizes the ratio of between-class covariance and within-class covariance.

$$S = \frac{\sigma^2_{between}}{\sigma^2_{within}} = \frac{(w^T(\mu_1-\mu_2))^2}{w^T(c_1+c_2)w} \quad (26)$$

For P300 signal classification, we used the LDA. For this purpose, three runs of the four experimental sessions are considered as training data, and the data recorded in runs four to seven are considered as test data. The data classes are set to 1 and 0, meaning that if the target is detected in the selected channel, that channel is classified as group 1, otherwise it is classified as group 0. To determine which class the data belongs to, we need to maximize the likelihood function. First, we find α, β, and weight vector W, then we maximize the conditional probability and obtain the mean and variance to determine the desired class for ensuring the accuracy of the classifier's performance using test data as in[51].

STATICAL ANALYSIS

The purpose of the statistical analysis was to test the hypothesis regarding the impact of sublayers such as age, disease stage on the performance of the P300 speller task and the extracted P300 features in the three executed methods, as well as the target detection time in each method.

Due to the small sample size, the Shapiro-Wilk test was used to assess the normal distribution of the data. The classification accuracy in the LDA+HOSRDA and LDA+No Reduction methods, as well as the test time in LDA+HOSRDA and SVM, showed normal distribution, and therefore, Pearson's correlation coefficient was calculated. Additionally, the classification accuracy of the SVM classifier and the test time in the LDA+No Reduction method had a non-normal distribution. Hence, the non-parametric Spearman correlation was used for analysis.

Given the small number of data points, further analysis was performed using ANOVA and t-tests for data with normal distribution, and the non-parametric Kruskal-Wallis test for data with non-normal distribution.

10.22060/EEJ.2025.24519.5721

5.Results

Characteristics of the study population was shown in table 1. Five ALS patients with an average age of 50.4 years (rangesfrom40 to 62 years) completed the study. The youngest patient was a 40-year-old woman, while and the oldest one was a 60-year-old man, with an average age at diagnosis of 48.2 years. The most common clinical presentation in these patients was spinal involvement (n: 4, 80%) (Table 1).

Table 1. Characteristics of the study population

Patient	Sex	Age	Age at diagnosis	Clinical manifestations	Onset of disorder	Family history of ALS	ALSFRS-R (ALS Functional Rating Scale-Revised)
1	F	62	60	Spinal	24 month	Negative	27
2	M	51	50	Spinal	6 month	Negative	34
3	M	51	49	Spinal	20 month	Negative	36
4	F	40	37	Spinal	36 month	Negative	27
5	M	48	45	Bulbar	36 month	Negative	22

All five patients successfully completed the BCI task phase. Additionally, fatigue was reported in three patients (60%) during task performance. Furthermore, none of the patients had prior experience with BCI. Specialized evaluations revealed that among the patients, the lowest ALSFRS-R score was 22 for the only patient with bulbar onset, and the highest score belonged to patient number 3, a 51-year-old male with spinal involvement and disease onset at age 49. The ALSFRS-R score for the oldest patient was 27. Among the four patients with spinal involvement, the ALSFRS-R score was 27 for two female patients, which was significantly lower than the scores of two male patients.

The Functional Rating Scale for ALS in its revised version (ALSFRS-R) is a disease-specific severity score that reflects motor impairment and functional decline in individuals with Amyotrophic Lateral Sclerosis (ALS). It is widely used in clinical research and ALS studies. Functional assessment through the ALSFRS-R is one of the most important outcomes in ALS

10.22060/EEJ.2025.24519.5721

clinical trials. In addition, this scale allows for modeling of individual disease progression and can predict survival.

Signal processing was optimized by using eight channels instead of all, and involved three preprocessing stages: low-pass, high-pass, and notch filtering to enhance performance and reduce processing time.

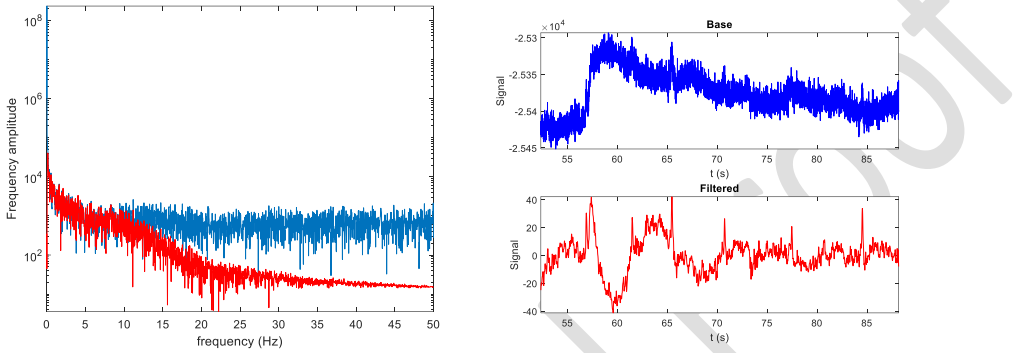

Figure8. Preprocessed signal of a trial at Cz in frequency domain (left) and time domain (right)

The data is segmented into 1000-ms epochs, with artifacts removed based on amplitude thresholds, and baseline corrections applied, followed by calculation of the P300 peak amplitude at Cz by comparing target and non-target epoch waveforms.

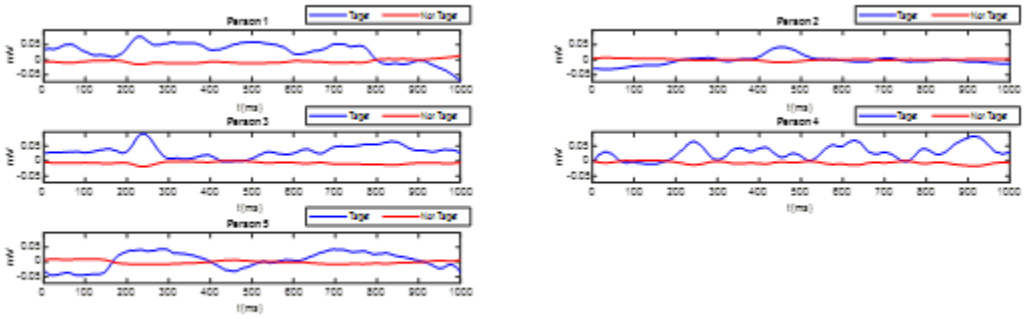

Figure ۹.EEG amplitude as a function of time in one trial for *N=5* participants.

As shown in table 2, the average classification accuracy obtained was 84.04%, which is promising for online use considering that training sessions and filters for age, disease severity, and literacy have not yet been implemented.

10.22060/EEJ.2025.24519.5721

Table 2. The accuracy of the classification of patients with amyotrophic lateral sclerosis

Patient	*ACC%* HOSRDA+LDA	Number of repeat	Test time	*ACC%* LDA, No reduction	Test time	*ACC%* SVM	Test time
1	82.41	3	0.001S	76.99	0.02S	83.80	0.03S
2	82.44	3	0.001S	77.44	0.004S	83.83	0.04S
3	83.18	3	0.001S	78.89	0.001S	83.66	0.03S
4	82.17	3	0.001S	78.83	0.001S	82.67	0.02S
5	82.35	3	0.001S	77.14	0.002S	83.77	0.03S

S: Second,

Based on the results, the HOSRDA+LDA method converges with very few repetitions and this is useful for online applications as the biggest challenge in online applications is reducing the time for analyzing high-volume data and sending commands to the external environment in real-time. Considering the importance of time in online BCI use, reducing the dimensions of multidimensional data analysis is of great importance, and the HOSRDA algorithm can be used samples. Additionally, the training time for HOSRDA is significantly less than support vector machine (SVM), and the computational complexity of solving linear equations is one of the advantages of using this algorithm. Based on the results of the scatter matrices in the first repetitions, convergence is achieved in the third repetition and due to the presence of a stability block, the system will maintain its stability (Table 3).

Table 3. The comparison of higher order spectral regression discriminant analysis (HOSRDA)+LDA and support vector machine (SVM) training time infivepatients with amyotrophic lateral sclerosis

Patient	HOSRDA+LDA	SVM
1	0.0031S	11.521S
2	0.0019S	6.041S
3	0.002S	3.37S
4	0.002S	3.066S
5	0.002S	5.32S

S: Second,

The HOSRDA method demonstrates efficiency by significantly reducing computational costs compared to traditional tensor methods. Its stability is an additional benefit, particularly in cases of ill-conditioned matrices. The application of HOSRDA to EEG data, such as from the P300 speller paradigm, highlights its superior performance in character detection tasks when compared to other tensor-based and machine learning methods.

Given the similar classification accuracy results between the **SVM** and **HOSRDA+LDA** methods, the **HOSRDA+SVM** method was specifically examined.

Table 4. The accuracy of the classification of patients with amyotrophic lateral sclerosis

Patient	ACC% HOSRDA+LDA	Number of repeat	Test time	Training Time	ACC% HOSRDA+SVM	Test time	Training Time
1	82.41	3	0.001S	0.0031S	83.81	0.027S	0.082S
2	82.44	3	0.001S	0.0019S	83.83	0.019S	0.090S
3	83.18	3	0.001S	0.002S	83.83	0.019S	0.035S
4	82.17	3	0.001S	0.002S	83.82	0.020S	0.084S
5	82.35	3	0.001S	0.002S	83.80	0.017S	0.096S

S: Second,

As can be seen, both methods achieve similar classification accuracy.
The training time for the **HOSRDA+LDA** method is very fast for each patient, ranging from 0.0019 seconds to 0.0031 seconds. This indicates that **HOSRDA+LDA** is much more efficient in terms of training time performance. It is highly time-efficient, and its high speed in training and testing makes it crucial for real-world performance.

On the other hand, **SVM**, due to the need for eigenvalue decomposition and complex computations during training, is computationally expensive, especially with large datasets. In contrast, **HOSRDA** is specifically designed to reduce computational complexity. By using regression instead of eigenvalue decomposition, its computational cost is reduced. Additionally, this method can solve complex computational problems using low-cost iterative algorithms.

Given the challenge of class imbalance in our data (with a 1:5 ratio between target and non-target classes), accuracy as the main evaluation metric cannot provide an accurate representation of model performance. Therefore, instead of accuracy, we have used F1-Score metrics, which are

more suitable for models with imbalanced data. Experimental results show that using these metrics has significantly improved the model's prediction quality.

“Across five independent sessions, the HOSDRA–LDA pipeline consistently achieved the highest performance, with F1-Scores of 0.6158, 0.6228, 0.6217, 0.6092, and 0.6229, and corresponding AUC values between 0.8892 and 0.8961. Notably, the recall remained 1.0 in all experiments, meaning that every target P300 response was successfully detected.

All SVM-based classifiers failed to provide reliable performance, frequently producing undefined F1-Scores or extremely low sensitivity. LDA without dimensionality reduction also demonstrated weaker performance across all sessions.

These results confirm that HOSDRA significantly enhances the discriminability of EEG-based P300 features and provides a highly stable and robust feature representation for LDA classification.” “Across five independent sessions, the HOSDRA–LDA pipeline consistently achieved the highest performance, with F1-Scores of 0.6158, 0.6228, 0.6217, 0.6092, and 0.6229, and corresponding AUC values between 0.8892 and 0.8961. Notably, the recall remained 1.0 in all experiments, meaning that every target P300 response was successfully detected.

All SVM-based classifiers failed to provide reliable performance, frequently producing undefined F1-Scores or extremely low sensitivity. LDA without dimensionality reduction also demonstrated weaker performance across all sessions.

These results confirm that HOSDRA significantly enhances the discriminability of EEG-based P300 features and provides a highly stable and robust feature representation for LDA classification.

Table5 :F1-Score for HOSRDA+LDA

Subject	Recall	AUC	F1
S1	1.00	0.8930	0.6158
S2	1.00	0.8961	0.6228
S3	1.00	0.8954	0.6217
S4	1.00	0.8892	0.6092
S5	1.00	0.8959	0.6229

we have added the complete Confusion Matrices and the corresponding True Positive Rate (Recall) and False Positive Rate (FPR) values for all competing methods (HOSRDA–LDA, LDA, and SVM) across all experimental sessions.

These results are now presented in a new table (Table X) and provide a clear comparison of classifier performance during the epoch classification stage.

We highlight that the HOSRDA–LDA method consistently achieved the highest Recall (1.00 across all sessions) and the lowest FPR among all methods, whereas SVM-based classifiers demonstrated poor sensitivity, often yielding Recall = 0.

Table 6 – Confusion Matrix, Recall, and FPR for HOSRDA+LDA (Best Method),S1

Metric	Value
TP	~493
FN	0
FP	Range (600-635) avg(607)
TN	Range (2230-2270) avg(2250)
Recall	1.0000
FPR	FP/(FP+TN) ~0.21-0.22
F1	≈0.6180
AUC	≈0.895

Table 7 – Confusion Matrix, Recall, and FPR for LDA (No Reduction),S1

Metric	Value
TP	~60
FN	~480
FP	~240
TN	~2550
Recall	0.14-0.10
FPR	≈0.08-0.09
F1	≈0.13-0.17

Table 8 – Confusion Matrix, Recall, and FPR for SVM (No Reduction),S1

Metric	Value
TP	0-15
FN	543-528
FP	0-38
TN	2779-2817
Recall	0.00-0.028
FPR	≈0.00-0.013
F1	0-0.05

Table 9 – Confusion Matrix, Recall, and FPR for HOSRDA+SVM,S1

Metric	Value
TP	0
FN	543
FP	0
TN	2817
Recall	0.00
FPR	0.00
F1	NaN

Table6,7,8,9 reports the Confusion Matrices together with the Recall (TPR) and FPR for all classifiers. The HOSRDA–LDA method achieved the highest Recall (1.00 across all five Subject) and a moderate FPR (~0.21), outperforming all competing approaches.

LDA without dimensionality reduction yielded lower Recall (0.10–0.14) and moderate FPR (~0.08–0.09).

LDA Classify demonstrated higher sensitivity (Recall 0.38–0.52) but at the cost of a substantially higher FPR (0.34–0.42).

SVM-based models consistently exhibited poor Recall (0.00–0.03), confirming their inadequacy for P300 detection under severe class imbalance.

Key features of the HOSRDA approach include:

- **Avoidance of Eigenvalue Decomposition**: This reduces the computational cost, especially for high-dimensional data, and handles ill-conditioned matrices effectively.
- **Regularization Flexibility**: Regularization terms, such as sparsity, can be easily incorporated into the regression formulation.
- **Efficiency for SSS Problems**: HOSRDA addresses the curse of dimensionality by simplifying data analysis without compromising performance.
- **Faster Convergence**: The method solves regression problems iteratively using low-complexity algorithms such as LSQR.

In conclusion, the HOSRDA method applied to EEG data from the P300 speller paradigm has shown promising results, with efficient classification and reduced processing time, making it a strong candidate for real-time BCI applications, particularly for individuals with ALS.

The goal of the statistical analysis was to test the hypothesis regarding the impact of sublayers such as age, disease stage on the performance of the P300 speller task and the extracted P300 features in the three executed methods, as well as the target detection time in each method.

Due to the small sample size, the Shapiro-Wilk test was used to assess the normal distribution of the data. The classification accuracy in the LDA+HOSRDA and LDA+No Reduction methods, as well as the test time in LDA+HOSRDA and SVM, showed normal distribution, and therefore, Pearson's correlation coefficient was calculated. Additionally, the classification accuracy of the SVM classifier and the test time in the LDA+No Reduction method had a non-normal distribution. Hence, the non-parametric Spearman correlation was used for analysis.

Given the small number of data points, further analysis was performed using ANOVA and t-tests for data with normal distribution, and the non-parametric Kruskal-Wallis test for data with non-normal distribution.

Pearson's correlation test was used to examine the linear relationship between ALSFRS-R and the classification accuracy of the classifiers (LDA+HOSRDA and LDA+No Reduction), while ANOVA was used to compare significant differences in the classification accuracy of the classifiers (LDA+HOSRDA and LDA+No Reduction) across different ALSFRS-R groups. A T-test was performed to compare the classification accuracy in the high and low ALSFRS-R groups.

Table 10 Pearson's Correlation Test Analysis

Method	Correlation Statistic *(r)*	*P-value*
ALSFRS-R vs LDA+HOSRDA	0.71	0.177
ALSFRS-R vs LDA+No reduction	0.47	0.426

A moderate correlation is observed between ALSFRS-R and LDA+HOSRDA, but this correlation is not statistically significant. Additionally, a weak correlation is observed between ALSFRS-R and LDA+No reduction, but given the P-value, it cannot be considered significant.

Table 11 ANOVA Test Analysis

Method	*F-statistic*	*P-value*
ALSFRS-R vs LDA+HOSRDA	2.95	0.184
ALSFRS-R vs LDA+No reduction	0.30	0.622

Based on the comparison of P-values in both groups, no significant differences can be observed between the ALSFRS-R (high and low) groups and the classification accuracy of the classifiers.

Table 12 T-test Analysis

Method	*T-statistic*	*P-value*
ALSFRS-R vs LDA+HOSRDA	1.72	0.184
ALSFRS-R vs LDA+No reduction	0.55	0.622

No significant differences were found between the high and low ALSFRS-R groups in this case as well. Overall, based on the results of the Pearson's correlation, ANOVA, and T-test, it can be stated that there is no significant relationship or difference between ALSFRS-R and the classification accuracy of the classifiers.

Similarly, these tests were performed on the test time data. Pearson's correlation, ANOVA, and T-test statistical analyses were carried out, and since the test times in the LDA+HOSRDA method

are very close to each other, no significant relationship or difference with ALSFRS-R in the test time was observed. For SVM, weak correlation and non-significant differences in test times were observed between different ALSFRS-R groups.

Spearman's Correlation Test: To examine the non-linear and non-parametric relationship between ALSFRS-R and the classification accuracy of the SVM classifier.

Kruskal-Wallis Test: To examine significant differences in the classification accuracy of the SVM classifier across different ALSFRS-R groups (high and low groups).

In the Spearman's correlation test, the correlation coefficient ($r = 0.0513$) indicates a very weak relationship between ALSFRS-R and the classification accuracy of the SVM classifier. The P-value is 0.935, suggesting that this correlation is not statistically significant (P-value > 0.05).

In the Kruskal-Wallis test, the H-statistic is 0.3333, and the P-value is 0.564, indicating that there is no significant difference in the classification accuracy of the SVM classifier across different ALSFRS-R groups. The test for the test time in the LDA+No Reduction method also does not show any significant differences.

6.Discussion

The early presentation of ALS include movement difficulties and slowness, muscle weakness and loss of muscle power, repetitive automatic movements, and a significant decline in muscle performance. In some cases,. At present, palliative treatments such as anti-inflammatory drugs, antioxidants, and physiotherapy can control symptoms and improve the quality of life of the patients. Adequate care and support for patients with ALS can also help to improve their quality of life[2].

Patients with ALS suffer from gradual loss of muscle control due to the loss of central and peripheral motor neurons. The goal of a considerable number of studies is to provide communication tools that can improve the lives of these patients. BCIs are a technology that can measure and analyze brain signals to make them visible for communication with the external

10.22060/EEJ.2025.24519.5721

environment. For example, controlling a robot to type letters, controlling a wheelchair to navigate to a desired location, rehabilitation, and treatment are some examples that this technology can manage. In addition, BCI technology is useful for healthy individuals as well. For example, it can be used to control various electronic devices, change TV channels, and adjust air temperature and music volume just by thinking without body movement. BCI can also be used in games, military objectives, and helping elderly people. Therefore, this technology has significant positive economic and social effects[7].

Due to the importance of BCI, this study focuses on examining tensor-based methods and the accuracy and speed of classification in these methods to reduce analysis time for ALS patients to use BCIs in the real world without the need for time-consuming training sessions for users of all languages and literacy levels. The study results indicate that the HOSRDA feature reduction algorithm and LDA achieve an average character detection accuracy of 84.04%. The results were obtained under signal registration conditions without training sessions for each individual and without filters such as age, disease severity, and literacy level. Additionally, this performance has been compared with other feature reduction and classification methods and has shown better performance than other methods.

In this study, parameter J=7 has been used, and compared with the HOSRDA+LDA and SVM methods on dataset II, classification accuracy of 72.5% and 73.5% have been obtained for two individuals, respectively[39], which shows a considerable improvement in three repetitions in the present method.

In addition to motor impairments, patients with ALS may suffer from respiratory failure, disrupted sleep, and fatigue, which may limit their working memory and attention[52, 53]. However, it is still unclear how significant these findings are in a practical environment; some studies have shown that P300 vectors are comparable in healthy participants and ALS patients, while others have observed fewer vectors in ALS patients[20, 54]. Similarly, some studies have found long delays in ALS, while others have shown no differences[55, 56].

Holzet al. found that the use of BCI-based methods can improve the quality of life of patients with ALS[57]. This study also demonstrated the efficacy of these methods in patients with ALS, which makes it clear that it can improve the quality of life of these patients. Since these results were

obtained without time-consuming training sessions and without considering the role of literacy and other intervention factors, it can be said that this method is useful and effective for almost all patients with ALS regardless of their literacy level, age, and disease severity. Therefore, it can play a significant role in improving the hope and quality of life of these patients.

In this study, age and ALSFRS-R did not affect the performance accuracy and test time of the data.

This study demonstrated that brain-computer interface technology based on tensor methods holds promising potential as an assistive communication tool for ALS patients. Further optimization of the algorithm and comprehensive studies with larger sample sizes are essential. While the initial findings are encouraging, they could lead to the development of more effective communication solutions specifically designed to address the challenges faced by ALS patients.

In this study, we compared multiple methods for epoch classification in P300 Brain-Computer Interface (BCI) applications, focusing on HOSRDA + LDA, LDA, and SVM as the primary classifiers. A major point of comparison was the True Positive Rate (Recall) and False Positive Rate (FPR), which were evaluated across five experimental sessions. These metrics are critical for understanding the classifiers' ability to accurately detect target P300 responses while minimizing false positives.
Confusion Matrix Analysis:

The Confusion Matrices for each method reveal important details about the classifier's performance, particularly in the context of class imbalance:

HOSRDA + LDA:

This method consistently achieved the highest performance across all sessions, with Recall = 1.00 (i.e., the model successfully detected all target epochs). The False Positive Rate (FPR) was moderate (~0.21 – 0.22), indicating that while some non-target epochs were misclassified as target, the model still demonstrated a high level of sensitivity without overpredicting target epochs. The F1-Score for this method was stable at around 0.61–0.62 across all sessions, reflecting its strong ability to balance both precision and recall.

LDA (No Reduction):

The Recall for LDA without dimensionality reduction was relatively low, ranging between 0.10 – 0.14, indicating poor sensitivity to target epochs. The FPR for this method was moderate (~0.08 – 0.09), suggesting that while the model detected some non-target epochs correctly, it still struggled

with detecting the target P300 responses. The F1-Score was consistently low (~0.13–0.18), reinforcing the model's poor ability to distinguish between target and non-target epochs.

LDA Classify:

The Recall for LDA Classify was higher than the non-reduced LDA method, ranging between 0.38 – 0.52, showing that the method detected a larger proportion of target epochs. However, the FPR was significantly higher (~0.34 – 0.42), indicating that the model misclassified a substantial portion of non-target epochs as targets. This led to a moderate F1-Score (~0.25–0.30), which highlights the trade-off between improved recall and a higher false positive rate.

SVM (No Reduction):

The SVM-based models consistently exhibited poor performance, with Recall = 0.00 – 0.03 in all sessions. This confirms that SVM is inadequate for P300 detection in this context, especially under conditions of severe class imbalance. The FPR for SVM was relatively low (~0.00–0.013), but this is largely due to its failure to predict target epochs accurately. As a result, F1-Score for SVM remained at 0, highlighting its ineffectiveness for this task.

Importance of HOSDRA:

A key contribution of this study is the integration of HOSDRA (Higher Order Spectral Regression Discriminant Analysis) for dimensionality reduction, which significantly enhanced the feature representation for LDA classification. By applying HOSDRA, the Recall was maximized at 1.00, ensuring that all target epochs were detected without failure. This reduction in dimensionality allowed for better computational efficiency and feature clarity, particularly when compared to standard LDA and SVM.

Impact on Classification Accuracy:

The HOSDRA + LDA method not only outperformed other classifiers in terms of Recall and FPR, but it also demonstrated superior AUC values (around 0.89 – 0.90), indicating strong discriminative power. While LDA Classify and LDA showed moderate performance in detecting target epochs, they were still heavily affected by class imbalance, leading to a significant number of false positives. The combination of HOSDRA with LDA mitigated these issues, providing a more reliable and stable approach to P300 classification.

10.22060/EEJ.2025.24519.5721

7.Conclusion

In this study, a tensor-based feature reduction method called HOSRDA was used inpatientswithALS. HOSRDA is the higher order extension of SRDAand a solution to the eigenvalue decomposition problem in HODA against the regression problem. This method was used to reduce the features of P300 spelling data. By using the HOSRDA feature reduction algorithm and LDA, an average character detection accuracy of 84.04% was achieved. This result was obtained under signal registration conditions without training sessions for each individual and without considering filters such as age, disease severity, and literacy level. Additionally, this method has been compared with other feature reduction and classification methods and has shown better performance than other methods. This method converges in an average time of 2.04 seconds over three repetitions, which is much less than other methods that may require several hours of training.

results indicate that brain-computer interfaces based on tensors are promising as an assistive communication tool for ALS patients. However, considering the statistical population in this study and the exclusion of patient training sessions for the purpose of generalizing the results, further optimization of the algorithm and controlled studies with larger sample sizes are essential for improving its performance and efficiency, as well as identifying disease-related influencing factors.

In summary, HOSDRA + LDA is the most reliable method for P300 detection in brain-computer interface systems, demonstrating optimal performance in terms of Recall, FPR, F1-Score, and AUC across multiple sessions. This method ensures high sensitivity to target epochs while maintaining a reasonable false positive rate, making it a robust choice for real-time BCI applications. The comparison with other methods, particularly SVM, highlights the importance of dimensionality reduction techniques like HOSDRA for enhancing classification performance, especially when dealing with class imbalance.

Recommendations

It is suggested that in the future, the proposed method should also be evaluated on healthy individuals.

Acknowledgements

This work is technically with collaboration Tehran University of Medical Sciences Shariati Hospital, Rare Diseases Foundation Of Iran, National Brain Mapping Laboratory.

References

1. Verbaarschot, C., et al., *A visual brain-computer interface as communication aid for patients with amyotrophic lateral sclerosis.* Clinical Neurophysiology, 2021. **132**(10): p. 2404–2415.
2. Worms, P.M., *The epidemiology of motor neuron diseases: a review of recent studies.* Journal of the neurological sciences, 2001. **191**(1-2): p. 3–9.
3. Talbot, K., *Motor neurone disease.* Postgraduate medical journal, 2002. **78**(923): p. 513–519.
4. Pugliese, R., et al., *Emerging technologies for management of patients with amyotrophic lateral sclerosis: from telehealth to assistive robotics and neural interfaces.* Journal of Neurology, 2022. **269**(6): p. 2910–2921.
5. Chaudhary, U., N. Mrachacz-Kersting, and N. Birbaumer, *Neuropsychological and neurophysiological aspects of brain-computer-interface (BCI) control in paralysis.* The Journal of physiology, 2021. **599**(9): p. 2351–2359.
6. Majmudar, S., J. Wu, and S. Paganoni, *Rehabilitation in amyotrophic lateral sclerosis: why it matters.* Muscle & nerve, 2014. **50**(1): p. 4–13.
7. Choi, W.-S. and H.-G. Yeom, *Studies to Overcome Brain–Computer Interface Challenges.* Applied Sciences, 2022. **12**(5): p. 2598.
8. De Venuto, D. and G. Mezzina, *A single-trial P300 detector based on symbolized EEG and autoencoded-(1D) CNN to improve ITR performance in BCIs.* Sensors, 2021. **21**(12): p. 3961.
9. Capogrosso, M., et al., *A brain–spine interface alleviating gait deficits after spinal cord injury in primates.* Nature, 2016. **539**(7628): p. 284–288.
10. Bonizzato, M., et al., *Brain-controlled modulation of spinal circuits improves recovery from spinal cord injury.* Nature communications, 2018. **9**(1): p. 3015.
11. Benabid, A.L., et al., *An exoskeleton controlled by an epidural wireless brain–machine interface in a tetraplegic patient: a proof-of-concept demonstration.* The Lancet Neurology, 2019. **18**(12): p. 1112–1122.
12. Han, X., J. Niu, and S. Guo, *A tactile-based brain computer interface P300 paradigm using vibration frequency and spatial location.* Journal of Medical and Biological Engineering, 2020. **40**: p. 773–782.
13. Zisk, A.H., et al., *P300 latency jitter and its correlates in people with amyotrophic lateral sclerosis.* Clinical Neurophysiology, 2021. **132**(2): p. 632–642.
14. Zhang, Z., et al., *Spatial-temporal neural network for P300 detection.* IEEE Access, 2021. **9**: p. 163441–163455.
15. Barthélemy, Q., et al., *End-to-end P300 BCI using Bayesian accumulation of Riemannian probabilities.* Brain-Computer Interfaces, 2023. **10**(1): p. 50–61.
16. Zani, A. and A.M. Proverbio, *Cognitive electrophysiology of mind and brain*, in *The cognitive electrophysiology of mind and brain*. 2003, Elsevier. p. 3–12.
17. Polich, J., *50+ years of P300: Where are we now?* Psychophysiology, 2020. **57**(7): p. e13616–e13616.
18. Fonken, Y.M., J.W. Kam, and R.T. Knight, *A differential role for human hippocampus in novelty and contextual processing: Implications for P300.* Psychophysiology, 2020. **57**(7): p. e13400.

19. Näätänen, R., et al., *The mismatch negativity (MMN) in basic research of central auditory processing: a review.* Clinical neurophysiology, 2007. **118**(12): p. 2544–2590.
20. Harris, J.J., R. Jolivet, and D. Attwell, *Synaptic energy use and supply.* Neuron, 2012. **75**(5): p. 762–777.
21. Proverbio, A.M., E. Camporeale, and A. Brusa, *Multimodal recognition of emotions in music and facial expressions.* Frontiers in human neuroscience, 2020. **14**: p. 32.
22. Herron, J.E., A.H. Quayle, and M.D. Rugg, *Probability effects on event-related potential correlates of recognition memory.* Cognitive Brain Research, 2003. **16**(1): p. 66–73.
23. Onishi, A., et al. *Tensor classification for P300-based brain computer interface*. in *2012 IEEE international conference on acoustics, speech and signal processing (ICASSP)*. 2012. IEEE.
24. Karlsson, L., et al., *Tensor decomposition of EEG signals for transfer learning applications.* Brain-Computer Interfaces, 2024. **11**(4): p. 178–192.
25. Li, J., et al., *A prior neurophysiologic knowledge free tensor-based scheme for single trial EEG classification.* IEEE Transactions on Neural Systems and Rehabilitation Engineering, 2008. **17**(2): p. 107–115.
26. Lan, T., *Feature extraction feature selection and dimensionality reduction techniques for brain computer interface.* Doctor of Philosophy in Electrical Engineering examined and approved thesis. Oregon Health & Science University, OHSU Digital Commons, Scholar Archive, Paper, 2011. **706**.
27. Karahan, E., et al., *Tensor analysis and fusion of multimodal brain images.* Proceedings of the IEEE, 2015. **103**(9): p. 1531–1559.
28. Cong, S., et al., *Comprehensive review of Transformer-based models in neuroscience, neurology, and psychiatry.* Brain-X, 2024. **2**(2): p. e57.
29. Abed-Meraim, K., N.L. Trung, and A. Hafiane, *A contemporary and comprehensive survey on streaming tensor decomposition.* IEEE Transactions on Knowledge and Data Engineering, 2022. **35**(11): p. 10897–10921.
30. Lotte, F., et al., *A review of classification algorithms for EEG-based brain–computer interfaces: a 10 year update.* Journal of neural engineering, 2018. **15**(3): p. 031005.
31. Cong, F., et al., *Tensor decomposition of EEG signals: a brief review.* Journal of neuroscience methods, 2015. **248**: p. 59–69.
32. Cyganek, B., et al., *A survey of big data issues in electronic health record analysis.* Applied Artificial Intelligence, 2016. **30**(6): p. 497–520.
33. Qiu, X. and Y. Zhang. *A traffic speed imputation method based on self-adaption and clustering*. in *2019 IEEE 4th International Conference on Big Data Analytics (ICBDA)*. 2019. IEEE.
34. Zhou, R., et al., *De-noising of magnetotelluric signals by discrete wavelet transform and SVD decomposition.* Remote Sensing, 2021. **13**(23): p. 4932.
35. Küçükaşcı, E.Ş., M.G. Baydoğan, and Z.C. Taşkın, *Multiple instance classification via quadratic programming.* Journal of Global Optimization, 2022: p. 1–32.
36. He, H., et al., *Principal component analysis and Fisher discriminant analysis of environmental and ecological quality, and the impacts of coal mining in an environmentally sensitive area.* Environmental monitoring and assessment, 2020. **192**: p. 1–9.
37. Aghili, S.N., et al., *A spatial-temporal linear feature learning algorithm for P300-based brain-computer interfaces.* Heliyon, 2023. **9**(4).
38. Zhang, Y., et al., *Spatial-temporal discriminant analysis for ERP-based brain-computer interface.* IEEE Transactions on Neural Systems and Rehabilitation Engineering, 2013. **21**(2): p. 233–243.
39. Idaji, M.J., M.B. Shamsollahi, and S.H. Sardouie, *Higher order spectral regression discriminant analysis (HOSRDA): A tensor feature reduction method for ERP detection.* Pattern Recognition, 2017. **70**: p. 152–162.

40. Yan, S., et al. *Discriminant analysis with tensor representation*. in *2005 IEEE Computer Society Conference on Computer Vision and Pattern Recognition (CVPR'05)*. 2005. IEEE.
41. Holz, E.M., et al., *Long-term independent brain-computer interface home use improves quality of life of a patient in the locked-in state: a case study.* Archives of physical medicine and rehabilitation, 2015. **96**(3): p. S16–S26.
42. Ramos-Murguialday, A., et al., *Proprioceptive feedback and brain computer interface (BCI) based neuroprostheses.* 2012.
43. Grosse-Wentrup, M., D. Mattia, and K. Oweiss, *Using brain–computer interfaces to induce neural plasticity and restore function.* Journal of neural engineering, 2011. **8**(2): p. 025004.
44. Jiang, N., et al., *An accurate, versatile, and robust brain switch for neurorehabilitation.* Brain-Computer Interface Research: A State-of-the-Art Summary 3, 2014: p. 47–61.
45. Christoph, G., B. Allison, and G. Edlinger, *Brain-Computer Interface Research: A State-of-the-Art Summary*. 2013, Springer.
46. Chistoph Guger, B. and E. Leuthardt, *Brain-computer interface research: a state-of-the-art summary-2.* Biosystems & biorobotics. 1st ed. NY—Berlin—Heidelberg: Springer, 2014. **6**.
47. Zhang, S., et al., *Application of a common spatial pattern-based algorithm for an fNIRS-based motor imagery brain-computer interface.* Neuroscience letters, 2017. **655**: p. 35–40.
48. Carvalho, M.D. and M. Swash, *Awaji diagnostic algorithm increases sensitivity of El Escorial criteria for ALS diagnosis.* Amyotrophic Lateral Sclerosis, 2009. **10**(1): p. 53–57.
49. Krusienski, D.J., et al., *Toward enhanced P300 speller performance.* Journal of neuroscience methods, 2008. **167**(1): p. 15–21.
50. Chatrian, G.E., E. Lettich, and P.L. Nelson, *Ten percent electrode system for topographic studies of spontaneous and evoked EEG activities.* American Journal of EEG technology, 1985. **25**(2): p. 83–92.
51. Cruz, A., G. Pires, and U.J. Nunes, *Double ErrP detection for automatic error correction in an ERP-based BCI speller.* IEEE transactions on neural systems and rehabilitation engineering, 2017. **26**(1): p. 26–36.
52. Strong, M.J., et al., *Consensus criteria for the diagnosis of frontotemporal cognitive and behavioural syndromes in amyotrophic lateral sclerosis.* Amyotrophic Lateral Sclerosis, 2009. **10**(3): p. 131–146.
53. Schneider, C., S. Fulda, and H. Schulz, *Daytime variation in performance and tiredness/sleepiness ratings in patients with insomnia, narcolepsy, sleep apnea and normal controls.* Journal of sleep research, 2004. **13**(4): p. 373–383.
54. Hammer, A., et al., *A neurophysiological analysis of working memory in amyotrophic lateral sclerosis.* Brain research, 2011. **1421**: p. 90–99.
55. McCane, L.M., et al., *P300-based brain-computer interface (BCI) event-related potentials (ERPs): People with amyotrophic lateral sclerosis (ALS) vs. age-matched controls.* Clinical Neurophysiology, 2015. **126**(11): p. 2124–2131.
56. Volpato, C., et al., *Working memory in amyotrophic lateral sclerosis: auditory event-related potentials and neuropsychological evidence.* Journal of Clinical Neurophysiology, 2010. **27**(3): p. 198–206.
57. Holz, E.M., L. Botrel, and A. Kübler, *Independent home use of Brain Painting improves quality of life of two artists in the locked-in state diagnosed with amyotrophic lateral sclerosis.* Brain-Computer Interfaces, 2015. **2**(2-3): p. 117–134.